

Paleoclimate Studies on Bykovsky Peninsula, North Siberia - Hydrogen and Oxygen Isotopes in Ground Ice

by Hanno Meyer¹, Alexander Yu. Dereviagin², Christine Siegert¹ and Hans-W. Hubberten¹

Summary: In wide areas of Northern Siberia, glaciers have been absent since the Late Pleistocene. Therefore, ground ice and especially ice wedges are used as archives for paleoclimatic studies. In the present study, carried out on the Bykovsky Peninsula, eastern Lena Delta, we were able to distinguish ice wedges of different genetic units by means of oxygen and hydrogen isotopes. The results obtained by this study on the Ice Complex, a peculiar periglacial phenomenon, allowed the reconstruction of the climate history with a subdivision of a period of very cold winters (60-55 ka), followed by a long stable period of cold winter temperatures (50-24 ka). Between 20 ka and 11 ka, climate warming is indicated in stable isotope compositions, most probably after the Late Glacial Maximum. At that time, a change of the marine source of the precipitation from a more humid source to the present North Atlantic source region was assumed. For the Ice Complex, a continuous age-height relationship was established, indicating syngenetic vertical ice wedge growth and sediment accumulation rates of 0.7 m/ky. During the Holocene optimum, ice wedge growth was probably limited due to the extensive formation of lacustrine environments. Holocene ice wedges in thermokarst depressions (alases) and thermoerosional valleys (logs) were formed after climate deterioration from about 4.5 ka until the present. Winter temperatures were warmer at this time as compared to the cooler Pleistocene. Migration of bound water between ice wedges and segregated ice may have altered the isotopic composition of old ice wedges. The presence of ice wedges as diagnostic features for permafrost conditions since 60 ka, implies that a large glacier extending over the Laptev Sea shelf did not exist. For the remote non-glaciated areas of Northern Siberia, ice wedges were established as a powerful climate archive.

Zusammenfassung: Weite Gebiete des nördlichen Sibiriens sind seit dem späten Pleistozän weitgehend frei von Gletschern. Als Archive für die Paläo-Klimaforschung wurde daher das Grundeis, und insbesondere Eiskeile, genutzt, die in der sibirischen Arktis weitverbreitet sind. Die Ergebnisse der Untersuchungen an Eis-Komplexen, einem besonderen kryolithogenetischen Phänomen, spiegeln die Klimageschichte der letzten 60.000 Jahre wider. Auf der Bykovski-Halbinsel östlich des Lena-Deltas konnten Eiskeil-Generationen aus verschiedenen genetischen Einheiten mittels stabiler Sauerstoff- und Wasserstoff-Isotope unterschieden werden. Eine Phase sehr kalter Winter (60-55 ka) kann von einer langen und stabilen Phase (50-24 ka) kalter Winter-temperaturen unterschieden werden. Für den Eis-Komplex können syngenetisches Eiskeil-Wachstum und eine kontinuierliche Sediment-Akkumulationsrate von etwa 0,7 m/1000 Jahre nachgewiesen werden. Die Isotopendaten zeigen, dass zwischen 20-11 ka eine Klima-Erwärmung stattfand, vermutlich nach dem letzten glazialen Maximum. Zu dieser Zeit fand eine Änderung der Bedingungen in den Niederschlags-Quellgebieten von einer feuchteren Quelle zur heutigen nordatlantischen Niederschlagsquelle statt. Das Eiskeilwachstum war während des holozänen Klimaoptimums vermutlich eingeschränkt, da zu dieser Zeit eine intensive Bildung von Thermokarst-Seen stattfindet. Erst nach einer Klima-Verschlechterung vor etwa 4.500 Jahren können sich bis in die heutige Zeit holozäne Eiskeile in Thermokarst-Senken (Alassen) und Thermoerosions-Tälern (Logs) bilden. Die Wintertemperaturen sind jedoch deutlich wärmer im Vergleich zum Pleistozän. Die Migration von Wasser zwischen Eiskeilen und dem Segregationseis kann die Isotopenzusammensetzung von Eiskeilen verändern, was bei der Klima-Interpretation berücksichtigt werden muss. Eiskeile sind auf Permafrostregionen beschränkt. Daher belegen die Eiskeile, die für die letzten 60.000 Jahre im Arbeitsgebiet nachgewiesen werden konnten, dass in dieser Zeit kein Schelf-Gletscher im Gebiet der Laptevsee existierte. In den nichtvergletscherten Gebieten der sibirischen Arktis können Eiskeile als bedeutende Klima-Archive genutzt werden.

INTRODUCTION

Hydrogen and oxygen isotopes are well known as useful tools for paleoclimatic studies in ice bodies, especially for paleo-temperature reconstruction and for the identification of the precipitation source (MERLIVAT & JOUZEL 1979). During the last 30 years, many efforts have been made in isotopic analysis of the ice caps of Greenland and Antarctica in order to provide information about climate changes through time (e.g. JOHNSEN et al. 1972, OESCHGER 1985, PETIT et al. 1999). In most parts of the Eurasian Arctic, glacier ice cores are not available and therefore, other climatic archives have to be considered for paleoclimatic reconstruction. This study is included in the German-Russian scientific co-operation project „System Laptev Sea 2000“ as a part of the multidisciplinary research program „Paleoclimate signals in ice-rich permafrost“. The main goals of the research program are the reconstruction of the paleoclimatic and paleoenvironmental conditions in ice-rich permafrost areas of Northern Siberia.

On the Bykovsky Peninsula, 50 km SE of the Lena Delta, NE Siberia, huge polygonal ice wedge systems within very ice-rich sediments, the so-called „Ice Complex“ were analysed. The Ice Complex is widely distributed in Northern Siberia (ROMANOVSKIJ 1985), especially in the coastal lowlands and along rivers like Lena, Yana or Indigirka. In Northern Canada, an equivalent of the Ice Complex is described for a few limited areas of the MacKenzie and Yukon river basins (FRENCH 1996). The Ice Complex is a special syncryogenic feature formed under severe climatic conditions, and it is a clue for non-glaciated areas. In these areas, precipitation is bound in ground ice instead of glacier ice.

Ground ice, defined as all types of ice contained in frozen or freezing ground (INTERNATIONAL PERMAFROST ASSOCIATION 1998), is fed by meteoric water sources. Therefore, ground ice can be studied as a paleoclimatic archive using stable isotope methods (MACKAY 1983, VAIKMÄE 1989, VAIKMÄE 1991, VASIL'CHUK 1991) similar to that in glaciers and ice caps. Oxygen isotope data of ground ice are commonly also used for the distinction of genetically different types of (ground) ice (VAIKMÄE 1991), for a stratigraphic subdivision of permafrost (ARKHANGELOV et al. 1986) or for the identification of thaw unconformities (BURN et al. 1986). Our studies focus on a combination of H and O isotopes, which extends the possibility to understand the processes leading to ground ice formation considerably. The application of hydrogen and oxygen isotopes to ground ice is used for a stratigraphic subdivision of the Ice Complex and for a reconstruction of the paleoclimatic variations for the last 60 ka.

¹ Alfred Wegener Institute for Polar and Marine Research, Research Unit Potsdam, Telegrafenberg A43, 14473 Potsdam, Germany. <hmeyer@awi-potsdam.de>

² Faculty of Geology, Moscow State University, 119899 Moscow, Russia.

THE WORKING AREA

The Bykovsky Peninsula is situated approximately 50 km SE of the Lena Delta, Northern Siberia, between 71° 40' - 71° 80' N and 129° 00' - 129° 30' E (Fig. 1). The study area is part of the coastal lowlands of the Laptev Sea region with continuous permafrost up to 500-600 m in thickness (YERSHOV 1989). The highest areas of the Bykovsky Peninsula reach about 40 m a.s.l. and are occupied by the Ice Complex. According to radiocarbon ages, its formation started about 60 ka BP (SCHIRRMESTER et al. submitted).

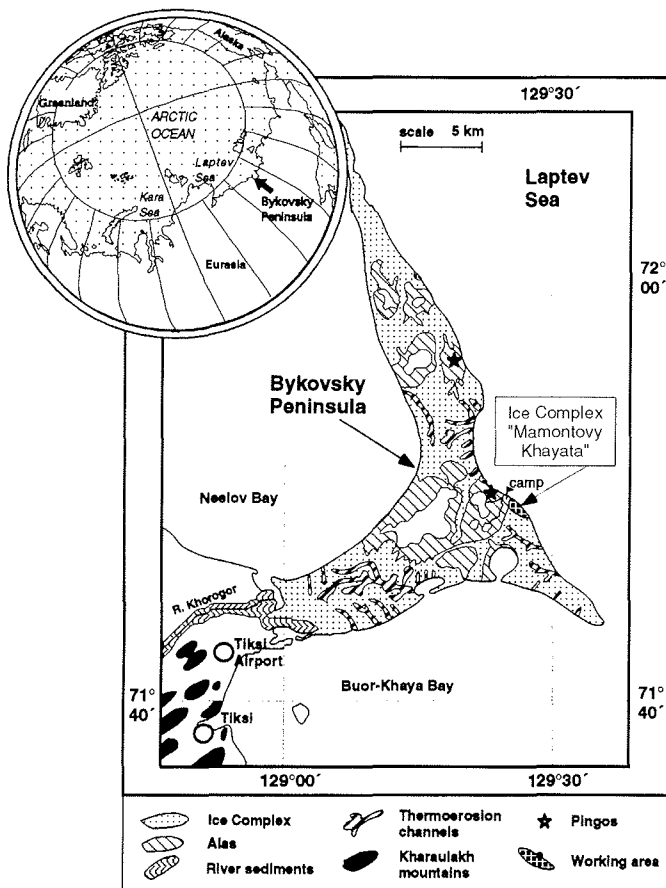


Fig. 1: Schematic map and geomorphological situation of the Bykovsky Peninsula.

Abb. 1: Schematische Karte und geomorphologische Situation der Bykovski-Halbinsel.

The genesis of the Ice Complex is still a matter of debate. Some authors explain the origin of the Ice Complex as part of a former alluvial plain (SLAGODA 1993), as fluvial (NAGAOKA 1994), others as cryogenic-eolian (TOMIRDIARO et al. 1984), as linked to nival processes of snow patches (KUNITSKY 1989), formed in ice-dammed lakes in front of shelf glaciers (GROSSWALD 1998) or as polygenetic (SHER et al. 1987).

The present climatic situation of the Bykovsky Peninsula can be drawn from the closest meteorological station in Tiksi (71° 35' N, 128° 55' E; NOAA data archive). The mean annual precipitation and temperature calculated for a 7-year period (1994

to 2000), are 400 mm and -12.2 °C, respectively. Additionally, NOAA provides mean annual precipitation data from 1932 to 1988 indicating a much lower precipitation of approximately 191 mm/yr. Thus, the considered 7-year period may have been particularly moist. The main period of precipitation is between June and September, with more than 60 % of the annual volume. Severe winters and short cold summers are typical for the region. The coldest month is January (mean temperature -31.3 °C), the warmest month is July (mean temperature 7.8 °C). Mean daily temperatures as low as -42.0 °C and as high as 18.0 °C were measured, pointing to a highly continental climate despite of the proximity of the Laptev Sea. The study area belongs to the Northern Tundra (ATLAS ARKTIKI 1985).

Vast areas of the Bykovsky Peninsula are covered by the Ice Complex, which is subject to thermoabrasion at the Laptev Sea coast and to different thermoerosional and thermokarst processes (Fig. 1). Thermokarst depressions (or alas) are frequent geomorphologic features and some still contain residual thermokarst lakes, usually less than 2 m deep. The Ice Complex on the Bykovsky Peninsula is subject to thermoerosion by small streams (or logs), forming characteristic steep gullies as well as wide and shallow valleys. A single, 28 m high pingo was observed in a large alas (Fig. 2).

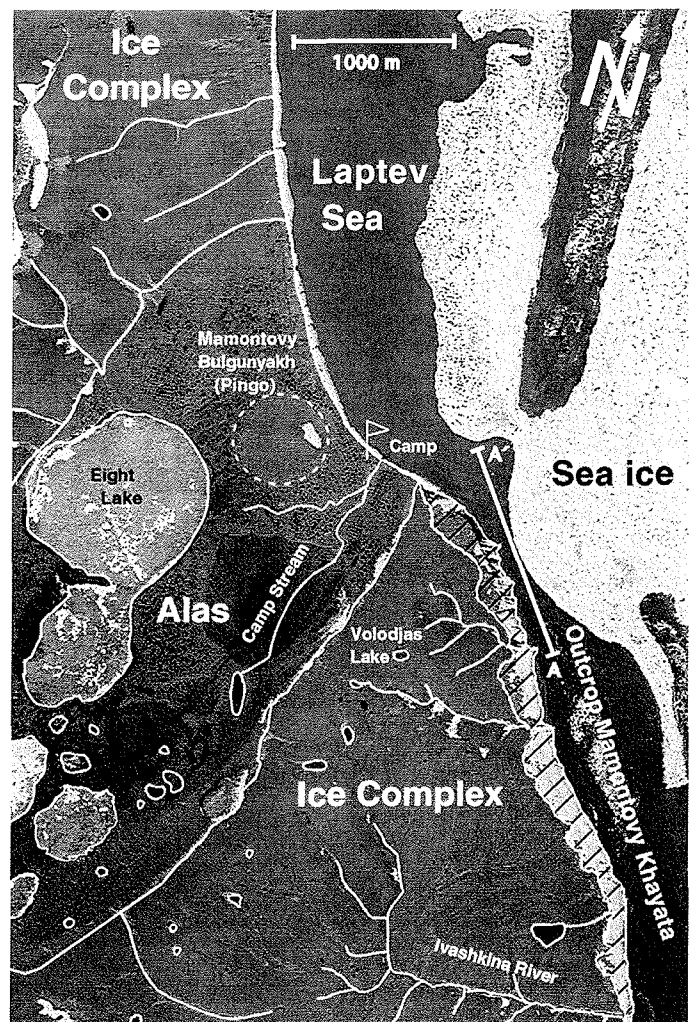


Fig. 2: Air photograph of the working area at the east coast of the Bykovsky Peninsula.

Abb. 2: Luftbild des Arbeitsgebietes an der Ostküste der Bykovski-Halbinsel.

THE OUTCROP

The Laptev Sea coast of Bykovsky Peninsula is characterised by steep cliffs and wide shallow terraces containing numerous thermokarst mounds (or baydzeraaks). The main part of the field work was carried out at a 1.5 km long and 40 m high coastal outcrop, called „Mamontovy Khayata“ (Mammoth mountain) located at the east coast of the peninsula (Fig. 3).

The outcrop is subdivided into three very ice-rich cryolithogenic facies with different types of ground ice and sediment: a 40 m high vertical profile of the Ice Complex and two younger genetic units, alas and log. All facies show ice wedge growth and fine dispersed segregated ice, and are covered by a 0.2-0.5 m thick active layer. The oldest genetic unit is the Ice Complex. It is characterised by relatively uniform loess-like silty sediments and a belt-like cryogenic structure. The alternation of massive ice belts and sediment layers with a lens-like reticulated cryogenic structure both turned upward near ice wedges point to syngenetic freezing. The ice wedges may reach widths of 5 m and heights of more than 40 m and the ice wedge tips are not found in the outcrop. Dirty, grey-coloured ice wedges are characteristic for the Ice Complex. In the uppermost part of the outcrop (Fig. 3), a few milky white ice wedges (parts of MKh-4.6) were observed, which reflects a higher content of gas bubbles. The total volumetric ice content in the Ice Complex may exceed 80 %. Organic material is well-preserved and composed of autochthonous peat, insect and plant macrofossils and bones of mammals such as mammoth, horses, bison and rodents. SCHIRMEISTER et al. (submitted) subdivided the evolution of the Ice Complex into three stages: a lower (0-10 m a.s.l.), a middle (10-25 m a.s.l.) and an upper horizon (25-39 m a.s.l.). The middle horizon (50-28 ka) is characterised by up to 15 peaty soil layers, whereas the lower (60-50 ka) and upper (25-12 ka) horizons have lower contents of organic material and a more uniform composition.

In the field, two younger facies (likely of Holocene age) discordantly overlying the Ice Complex could be distinguished sedimentologically and by different ice wedge generations. The alas is located in the NW of the outcrop and shaped by a polygonal landscape with numerous low-centre polygons (Fig. 2). Medium-grained sands are covered by peat layers up to 1 m in thickness. Ice wedge formation began after progressive freeze-back of the unfrozen zone (talik) below a thermokarst lake (FRENCH 1996). Alas ice wedges are up to 3.6 m wide, more than 5 m high and extend beneath the sea level. Log deposits overly the Ice Complex in the SE and are characterised by fine-grained sands partly covered by peat. Log ice wedges are smaller in width (max. 1 m) and height (max. 3.5 m). All ice wedges formed in environments younger than the Ice Complex are characterised by a milky white appearance. In some parts of the outcrop, we observed ice veins penetrating the active layer, which is subject to annual freezing and thawing. This suggests active ice wedge growth in the Holocene genetic units alas and log.

SAMPLING STRATEGY

In the studied permafrost sequences of the Bykovsky Peninsula, mainly two types of ground ice were found: ice wedges and segregated ice. Additionally, pingo ice occurs in the alas. The most promising archives for paleoclimatic reconstructions are ice wedges, which are formed principally by frost cracking in the upper part of permafrost due to rapid cooling at very low winter temperatures (LACHENBRUCH 1962). During snow melt in spring, meltwater from the previous years' winter precipitation penetrates into the frost cracks, preferentially near the centre of the ice wedge and often at the same place (MACKAY 1974). The meltwater freezes immediately, due to the low permafrost temperatures (on the Bykovsky Peninsula presently ca. -10 °C). Repeated annual freezing leads to a succession of

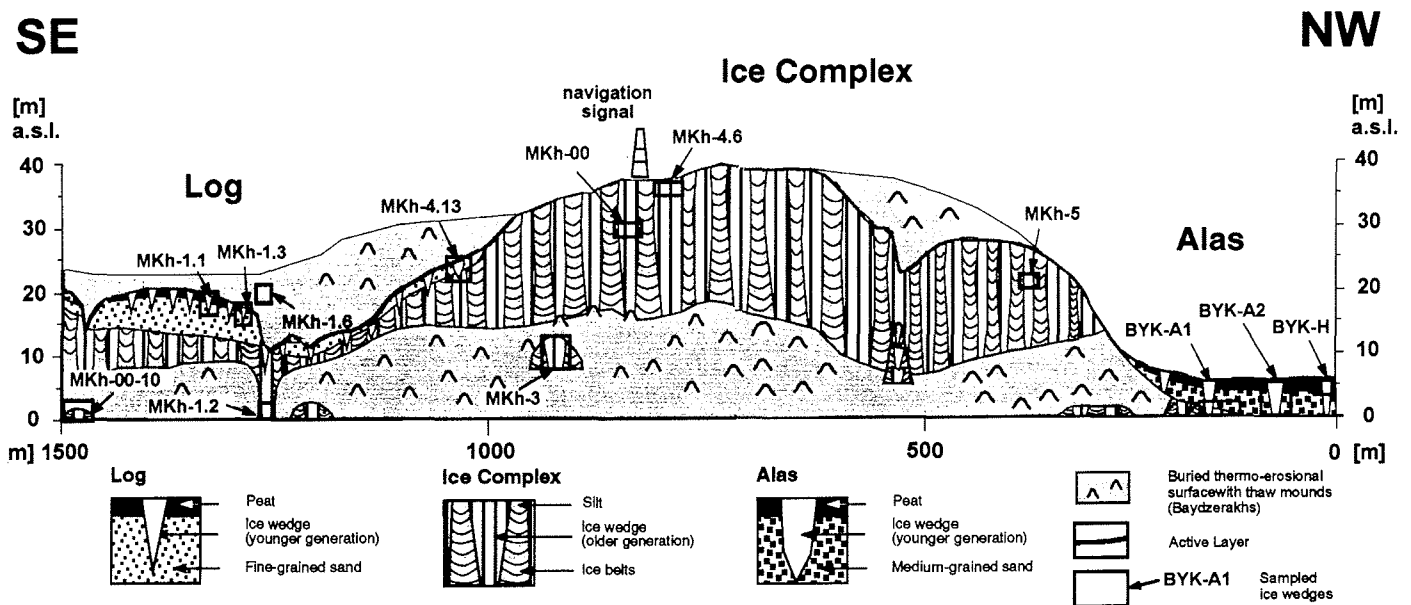


Fig. 3: Schematic profile of the outcrop "Mamontovy Khayata" (Mammoth mountain), east coast of Bykovsky Peninsula: Cryolithogenic units and the respective sampling locations for ice wedges.

Abb. 3: Schematisches Profil des Aufschlusses „Mamontovy Khayata“ (Mammutberg) an der Ostküste der Bykowski-Halbinsel: Kryolithogenetische Einheiten und Probenahme-Positionen für Eiskeile.

vertical veinlets and finally to the formation of an ice wedge. As a consequence of this process, in the ideal case, ice wedges get continuously older from the middle towards the margins. The ice wedges, which occur in the studied Ice Complex, also grew upward with the sediment accumulation. Therefore, sampling was performed both in vertical and in horizontal directions (Fig. 4). In addition, the contact zone between the ice wedge and the sediment was sampled carefully to identify possible exchange processes between the ice wedge and the frozen sediment.

Segregated ice can also be used for paleoclimatic studies despite fractionation processes, which may occur during freezing and despite the participation of different water sources in its formation. Sediment accumulation or climatic cooling both result in an upward movement of the lower boundary of the active layer. The lower part of the former active layer is transferred into perennially frozen sediments with segregated ice. Mixing of water from atmospheric precipitation, surface waters and meltwater occurs in the active layer, resulting in a homogenisation of the isotopic composition, the variations of which are due to changes in climatic or facial conditions (VAIKMÄE 1989).

The ground ice was sampled using an ice screw or a chain saw, and was thawed on site. Samples for ^{14}C dating, hydrogen and oxygen isotopes, tritium and hydrochemical analyses were taken for the whole vertical profile of the Ice Complex and for the Holocene genetic units, alas and log. For stable isotope and tritium analyses, meltwater was collected in 30 ml PE bottles, which were tightly closed to avoid evaporation (MEYER et al. 1999).

ANALYTICAL PROCEDURE

The H and O isotope measurements were carried out with a Finnigan MAT Delta-S mass spectrometer with two equilibration units. Both, oxygen ($^{18}\text{O}/^{16}\text{O}$) and hydrogen (D/H) isotopes ratios were analysed for the same water sample using common equilibration techniques (EPSTEIN & MAYEDA 1953). ^{17}O and H_3^+ corrections were carried out automatically. $^{18}\text{O}/^{16}\text{O}$ and D/H ratios are presented as $\delta^{18}\text{O}$ and δD . These δ values give the respective ‰-difference relative to the standard V-SMOW. The internal 1σ error is generally <0.8 ‰ for δD and <0.1 ‰ for $\delta^{18}\text{O}$, for all measurements (MEYER et al. 2000). Tritium (^3H), as radioactive hydrogen isotope was used as an indicator for the „modern water contamination“ in permafrost (CHIZHOV & DEREVIAGIN 1998) in order to check the validity of stable isotope analysis of ground ice. Tritium concentrations were determined at the Department of Radiochemistry, Moscow State University by a liquid-scintillation mass spectrometer Tricarb-1600 with an error of about 10 %. Electrical conductivity was measured with a WTW instrument.

AGE ESTIMATE OF THE ICE COMPLEX

The ages of the sediments in the outcrop were estimated by conventional and Accelerator Mass Spectrometry (AMS) ^{14}C dating of plant remains (SCHIRMEISTER et al. submitted). Figure 5 shows the continuous sedimentary evolution of the studied Ice Complex section between about 60 ka (at sea level) and 12.2 ka (at 37 m a.s.l.).

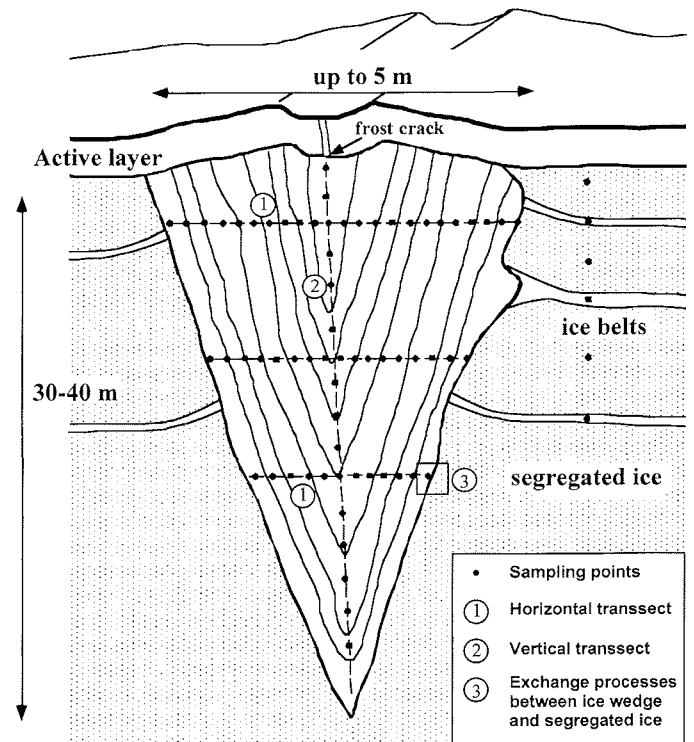


Fig. 4: Schematic sampling strategy for ground ice (ice wedges and segregated ice).

Abb. 4: Probenahmeschema für Grundeis (Eiskeile und Segregationeis).

In Table 1, new AMS ^{14}C ages of organic remains found in ice wedges and in sediments with direct contact to the sampled ice wedges are presented. All AMS ^{14}C age determinations were carried out in the Leibniz Laboratory in Kiel, Germany. Only leached residues were used. Since the abundance of organic material is quite low in the ice wedges, first direct AMS dating of micro-organic remains in the ice wedges was not published until recently (VASIL'CHUK et al. 2000). According to our experience bulk organic matter gets easily contaminated by younger material during sampling, whereas small leaves, twigs or lemming coprolithes proved to be less prone to contamination. To compare Pleistocene and Holocene samples, uncalibrated ^{14}C ages were used in Figures 5 and 9. Additionally, samples younger than 24 ka were calibrated after INTCAL98 (STUIVER et al. 1998) and given in Table 1.

In Figure 5, a linear relationship between all conventional and AMS ^{14}C ages in the Ice Complex sediments and the heights of the samples in the outcrop is indicated. The AMS ^{14}C ages of organic remains in ice wedges (e.g. for ice wedge MKh-3) are in general slightly younger than those for the enclosing sediment. This is probably due to the fact that frost cracks always penetrate into slightly older sediment. A Scheffé test shows that the new ages in ice wedges and in the host sediments belong statistically to the same population. Mean values and variances do not differ significantly at a probability of $p = 0.05$. Therefore, a linear age-height relationship was established based on all samples available. Accordingly, continuous ice wedge growth occurring syngenetically to the sedimentation is assumed for the outcrop (Fig. 5). The meaning of a continuous Ice Complex formation should not be

AMS dating of organic material close to ice wedges

Lab. Number	sample	material	genetic unit	height (m, a.s.l.)	¹⁴ C age BP [a]	+ [a]	- [a]	cal BP [a]	+2σ [a]	-2σ [a]
KIA 11442	MKh-4.6-14C-3	peat	Active Layer above Ice Complex	37.0	300	30	30	313	471	288
KIA 6722	MKh-1.6-2	peat	peat covering log deposits	17.2	1080	35	35	969	1063	927
KIA 6723	MKh-1.6-3	peat	peat covering log deposits	17.4	1105	35	35	986	1167	931
KIA 8161	MKh-4.12-3a	peat inclusion, horizon 5	peat in log deposits	26.0	4455	35	35	5045	5295	4871
KIA 6720	MKh-4.6-1	peat, plant remains, wood	uppermost part of Ice Complex	36.6	8230	50	50	9212	9424	9027
KIA 11441	MKh-4.6-14C-2	peat	uppermost part of Ice Complex	36.5	10840	50	50	12902	13116	12641
KIA 6721	MKh-4.12-2a	peat	Ice Complex	24.1	24460	250	260	-	-	-
KIA 6727	MKh-3	peat inclusion	Ice Complex	10.0	45090	2770	2060	-	-	-
KIA 6730	MKh-1.2-14C-1	peat, wood residues	Ice Complex	2.5	58400	4960	3040	-	-	-

AMS dating of organic material in ice wedges

Lab. number	sample	material	genetic unit	height (m, a.s.l.)	age [a]	+ [a]	- [a]	cal BP [a]	+ [a]	- [a]
KIA 6743	BYK-A2-89a	plant remains (BYK A2)	alas ice wedge	4.5	1220	35	35	1171	1264	1008
KIA 6742	BYK-A2-1-58	plant remains (BYK A2)	alas ice wedge	2.5	2075	35	35	2027	2149	1927
KIA 6744	BYK-A2-Be8/9	plant remains (BYK A2)	alas ice wedge	2.7	2370	30	30	2352	2704	2334
KIA 6741	BYK-A2-1-2	plant remains (BYK A2)	alas ice wedge	2.5	3075	40	40	3285	3382	3082
KIA 6747	MKh-4.6-1-47	plant/wood remains (MKh-4.6)	uppermost part of Ice Complex	36.4	9390	60	60	10613	11041	10425
KIA 11457	MKh-4.6-1-25	plant remains (MKh-4.6)	uppermost part of Ice Complex	36.4	11180	100	100	13151	13758	12893
KIA 6746	MKh-5-1-11	plant/wood remains (MKh-5)	Ice Complex	19.8	26050	190	190	-	-	-
KIA 8168	MKh-3-mouse	lemming coprolith (MKh-3)	Ice Complex	10.0	41990	1050	930	-	-	-

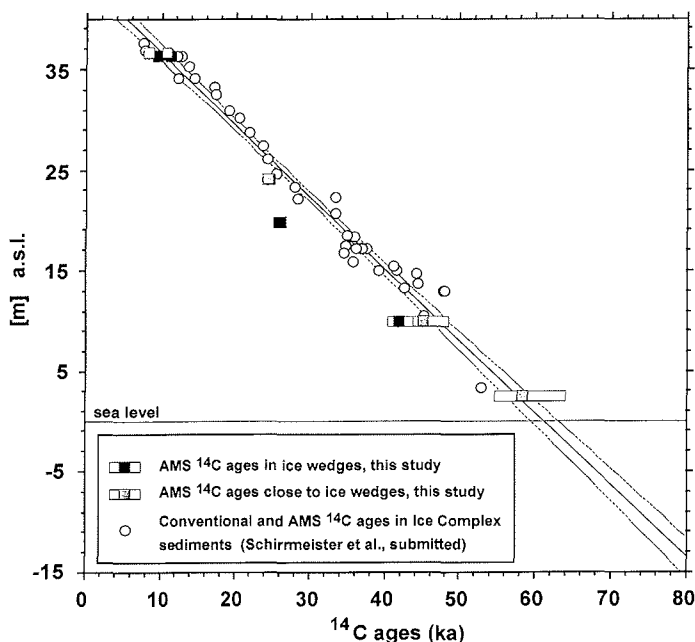
Tab. 1: New AMS ¹⁴C ages of organic material in ice wedges and in sediments enclosing ice wedges of the three genetic units Ice Complex, alas and log.

Tab. 1: Neue AMS ¹⁴C-Alter von organischem Material in Eiskeilen und im angrenzenden Sediment für die genetischen Einheiten Eis-Komplex, Alass und Log.

overestimated because changes in sedimentation rates (SCHIRRMESTER et al. submitted) and in vertical ice wedge growth can not be excluded. An approximate rate of Ice Complex evolution was assumed to be 0.7 m/kyr. The age-height relationship for vertical Ice Complex and ice wedge growth is:

$$T = 59.9 - 1.33 Z \quad (1)$$

where T denotes the age in ka and Z the height [m, a.s.l.]. The



coefficient of determination ($R^2 = 0.97$) represents a large part of the variation. VASIL'CHUK et al. (2000) calculated for Yamal a vertical ice wedge accumulation rate of 1.2-1.3 m/kyr. This larger accumulation rate is probably caused by a higher sedimentation rate. Our equation was used: (i) to estimate the age of ice wedges at our study site, which had not been dated up to now (BYK-A1, MKh-00, MKh-00-10), in order to include them into the paleoclimatic reconstruction, and (ii) to calculate the maximum age of the Bykovsky Ice Complex. Using equation (1), MKh-00 is 20 ka old, BYK-A1 59 ka and MKh-00-10 about 60 ka. Drilling of permafrost in the adjacent shelf near Bykovsky Peninsula has shown that the Ice Complex exists at 15 m below sea level (GRIGORYEV et al. 1996, ROMANOVSKIJ et al. 2000). Assuming continuous Ice Complex growth for the

Fig. 5: New AMS ¹⁴C ages of organic remains in ice wedges (black squares) and in the sediments in direct contact to the sampled ice wedges (grey squares) of the Ice Complex „Mamontovy Khayata“, with their respective error bars versus the height in the outcrop. White circles indicate conventional and AMS ¹⁴C ages of organic material in the sediment sampled without relation to ice wedges, as published by SCHIRRMESTER et al. (submitted). A Scheffé test has shown that ice wedge and sediment ages belong to the same population. Therefore, a linear correlation between ages and heights is given (straight line) based on all samples available including the 95 % confidence interval (dashed lines).

Abb. 5: Neue AMS ¹⁴C-Alter von organischem Material aus Eiskeilen (schwarze Quadrate) und aus dem Sediment in direktem Kontakt zu den beprobten Eiskeilen (graue Quadrate) für den Eis-Komplex „Mamontovy Khayata“, inklusive Fehlerbalken und Höhe im Aufschluss. Weiße Punkte kennzeichnen konventionelle und AMS ¹⁴C-Alter von organischem Material im Sediment nach SCHIRRMESTER et al. (eingereicht). Ein Scheffé-Test zeigt, dass Eiskeil- und Sediment-Alter statistisch der gleichen Grundgesamtheit entstammen. Aus den datierten Proben ergibt sich eine lineare Alters-Höhen-Beziehung (gerade Linie) mit 95 % Vertrauensintervall (gestrichelte Linie).

whole period of its formation, Ice Complex ground ice and sediment on Bykovsky Peninsula could be as old as 80 ky.

MACKEY (1992) reported that the frequency of ice wedge cracking was highly variable from 8 % to 75 %, for two nearby located sites on Garry Island, Canada between 1967 and 1987. Therefore, it is impossible to infer the age of an ice wedge by counting the annual ice veins. Nevertheless, it is possible to estimate ages. We observed single veinlets with mean widths of 2-2.5 mm, ranging between 1-4 mm. Thus, the sampling resolution (10 cm intervals) in our study corresponds to around 50, but certainly more than 25 and less than 100 cracking events between two horizontal samples. If we assume a frost cracking frequency of 75 % (rather high; for Ice Complex growth, cracking must have occurred relatively often), a minimum of 1 kyr, and an estimate of 2 kyr are needed for the growth of a 3 m wide ice wedge. For ice wedge MKh-4.6, an AMS ^{14}C age of 9.4 ka proves that ice wedge growth proceeded to the Early Holocene. This signifies that on this site, ice wedge growth continued after the end of Ice Complex sediment accumulation. An age of 11.2 ka in the same ice wedge shows that the growth of a horizontal transect of this ice wedge would take at least 1.8 ka.

AGE ESTIMATE OF THE HOLOCENE GENETIC UNITS

The AMS ^{14}C dating was also carried out for the Holocene units, alas and log (Tab. 1). All AMS ages of alas ice wedges were dated „directly“, whereas in log only organic matter in host sediments could be dated. For alas and log, no age-height relationship could be established. Therefore, all Holocene ice wedges, which could not be dated directly by AMS or ^3H methods, were put into a „logical“ order.

According to four AMS ages of organic remains, ice wedge BYK-A2 in the alas was formed in the interval from 3.1 ka to 1.2 ka, whereas the surrounding sediment is slightly older (SCHIRRMESTER et al. submitted). BYK-A1 and BYK-H have not been dated. However, BYK-A1 should be older than BYK-A2 because it was sampled at sea level, where the sediments are older and closer to the margin of the alas. BYK-H is located closer to the centre and was sampled at 5.1 m. Hence, it should be younger because it fell dry later. In the alas, active ice wedge growth was observed (Fig. 2).

Log sediments in the southern part of Mamontovy Khayata outcrop (MKh-4.13) were formed around 4.5 ka. The AMS data point to an age of the log-covering peat layer (MKh-1.6) of about 1 ka. Ice wedge growth should have started synchronous to or later than peat formation. Elevated tritium concentrations of ice veins (or „heads“) in the lowest part of the still frozen active layer (MKh-1.6, MKh-1.3) prove ice wedge growth during the last 50 years (DEREVIAGIN et al. 2002). MKh-1.1 belongs to the same ice wedge generation under the peat layer and is probably slightly older, because no tritium was detected. The occurrence of Holocene ice wedges is proved from around 3.1 ka until today (Tab. 1). From the Holocene warm period (8-5 ka), no ice wedges could be dated. This could be by chance or due to a missing ice wedge growth at the sampled sites in that time interval. The existence of large thermokarst lakes during the Holocene warm period may have prevented frost cracking at the studied sites.

RESULTS AND DISCUSSION

On a global scale, the δD and $\delta^{18}\text{O}$ of fresh surface waters are correlated linearly in the „Global Meteoric Water Line“ (GMWL). This relationship between δD and $\delta^{18}\text{O}$ is due to temperature-dependent fractionation at the phase transitions of water (evaporation, condensation, melting or freezing) in the hydrological cycle, and is defined as:

$$\delta\text{D} = 8 \delta^{18}\text{O} + 10 \text{‰ SMOW} \quad (\text{CRAIG } 1961) \quad (2)$$

The lowest $\delta^{18}\text{O}$ and δD values are attributed to the coldest temperatures. The ocean is the main source for atmospheric water vapour. The movement of an air mass from a moisture source towards higher latitude, altitude or distance to the sea progressively removes the heavy isotopes from the cloud. DANSGAARD (1964) introduced the deuterium excess (d) giving the position relative to the GMWL in a δD - $\delta^{18}\text{O}$ diagram, defined as:

$$d = \delta\text{D} - 8 \delta^{18}\text{O} \quad (\text{DANSGAARD } 1964) \quad (3)$$

d reflects the sensitivity of H and O isotopes to kinetic fractionation processes in the hydrological cycle. Being a function of the relative humidity, sea surface temperature and wind speed (MERLIVAT & JOUZEL 1979) in the moisture source region, d may be used for the identification of the source of precipitation.

RECENT PRECIPITATION

In Figure 6, the seasonal variation of recent precipitation is displayed in the $\delta^{18}\text{O}$ - δD diagram for rain water and snow patch samples of Bykovsky Peninsula. The scatter of precipitation data in the diagram reflects seasonal variations due to different condensation temperatures of water vapour out of the air mass. Mean, maximum and minimum isotopic compositions for rain and snow can be drawn from Table 2.

Samples of snow patches ($N = 9$) were taken during the field season in summer 1998 on Bykovsky Peninsula. Snow samples move along the GMWL, with a slope of 8.0 and an intercept of 9.6 points to the oceans being the main source for winter precipitation. A slope of 8.0 has also been described by BOIKE (1997) for snow in the Levinson-Lessing Lake area, Taymyr Peninsula. The combination of both studies reveals that sublimation, evaporation and melting of the snow did not lead to a significant change of d excess in the snow. Therefore, we can use these remnants of snow (already subject to melting) as our local source for ice wedge formation. Additionally, rain water ($N = 10$) was collected between 25 July and 17 August 1998. The samples are shifted from the GMWL towards a lower mean d excess of 2.7 ‰ and a smaller slope of 6.8. This enrichment in heavy isotopes is due to evaporation processes probably originating from surface waters or from the open Laptev Sea. Thus, winter and summer precipitation on Bykovsky Peninsula are of different origin, a phenomenon also described for the Taymyr Peninsula (BOIKE 1997). The similar pattern in the δD - $\delta^{18}\text{O}$ diagram of recent precipitation points to the same moisture source for both regions.

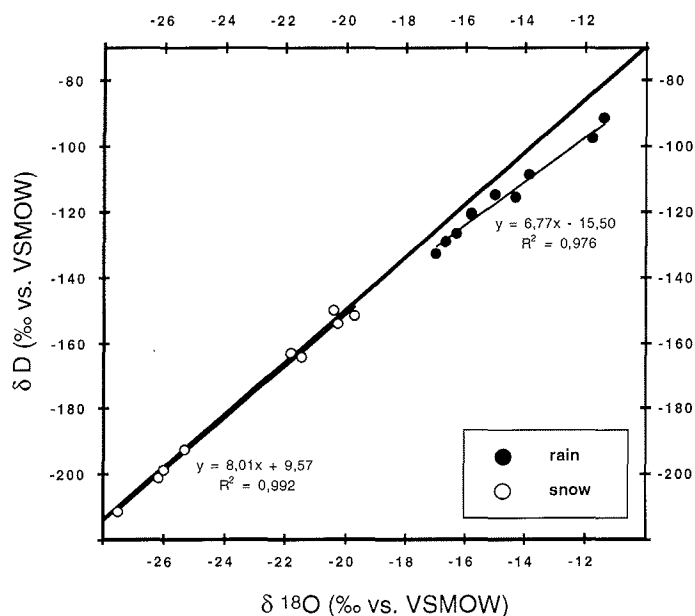


Fig. 6: $\delta^{18}\text{O}$ - δD diagram for samples from snow patches and rain collected in summer 1998 on Bykovsky Peninsula. GMWL is the Global Meteoric Water Line.

Abb. 6: $\delta^{18}\text{O}$ - δD -Diagramm für Schnee- und Wasserproben von der Bykovski-Halbinsel (Probenahme im Sommer 1998). GMWL ist die globale meteorische Wasserlinie.

STABLE ISOTOPES IN ICE WEDGES

Melting of snow is generally accepted as the main source for recent ice wedge ice (e.g. MACKAY 1983, VAIKMÄE 1989). Accordingly, the oxygen isotope composition of ice wedges was correlated with mean annual winter temperatures (VAIKMÄE 1991, VASIL'CHUK 1992). For the Bykovsky Peninsula, snow has been identified as the main source for modern ice wedges by DEREVIAGIN et al. (2001). For the interpretation of the ice wedge isotope data, the main area of interest is, which effects might influence $\delta^{18}\text{O}$ and δD in an ice wedge being a possible sink for water in the hydrological cycle. Mainly three groups of processes leading to a distinct stable isotope value in an ice vein must be considered: (i) fractionation processes at phase transitions of water in (winter) precipitation and in frost cracks, (ii) alteration of the isotopic signal in the ice wedge after its formation, (iii) different sources and pathways of water vapour including mixing.

The isotopic composition of discrete snowfall events is influenced by various processes from the formation of an air mass moving from a moisture source to the deposition site and influenced by changes in the atmospheric circulation (JOUZEL et al. 1997). Additionally, the seasonality of precipitation events within one year must be taken into account. Two climatically identical years might give different $\delta^{18}\text{O}$ in ice veins, e. g. when in one year, the frost crack is mainly fed by colder November snow and in the other by warmer March snow. Changes in seasonality of precipitation therefore have a great impact on stable isotopes and related paleothermometry (JOUZEL et al. 1997). Evaporation, sublimation and melting of a snow mass can be assumed to have a small effect on isotopes in the working area because the snow sampled in summer 1998 still shows a slope of 8 in the $\delta^{18}\text{O}$ - δD diagram, and

consequently has not been modified isotopically. Melting of the annual snow cover leads to the formation of one single elementary ice veinlet. This means a meteoric water line of snow is transferred into one point in the $\delta^{18}\text{O}$ - δD diagram. If we consider isotope fractionation for snow melting, the first melt water will have a lighter $\delta^{18}\text{O}$ and δD than the last. Additionally, mixing with water of different origin must be considered. At the time the snow starts melting, the active layer is still frozen and can therefore be ruled out as major source, but flooding may have an effect on ice wedges (especially at river and lake terraces).

The frequency of ice wedge cracking is highly variable (MACKAY 1992) and subject to seasonality. Cracking mainly tends to occur in winter between mid-January and mid-March (MACKAY 1974). For the growth of ice wedges, the existence of a thin snow cover is necessary, because of the insulating effect of the snow impeding frost cracking. When (melt) water enters frost cracks in spring, no fractionation takes place when the freezing process is faster than 2 mm/h, which is the critical value (MICHEL 1982).

Possible processes for the alteration of the isotope signal in an ice wedge after its formation are diffusion of water vapour and water migration due to gradients in hydrochemical composition. These effects may best be studied at the interface between ice wedge and segregated ice, which are both fed by waters of different origin. Here, a gradient in isotopic composition and in hydrochemistry can be expected. In Figure 7a-7c, the electrical conductivity, $\delta^{18}\text{O}$ and d are displayed for a 5 m long horizontal sampling transect across Pleistocene ice wedge MKh-3. The middle part of the ice wedge shows only slight variations in conductivity between 150-250 $\mu\text{S}/\text{cm}$. At the interface of the ice wedge and sediment, a higher conductivity of up to 530 $\mu\text{S}/\text{cm}$ was measured. The enclosing segregated ice is characterised by a much higher conductivity of up to 5500 $\mu\text{S}/\text{cm}$. For oxygen isotopes and d excess, a similar effect is observed. An isotopic composition of -22.5 ‰ in $\delta^{18}\text{O}$ and low d of -6 ‰ are measured close to the edges of the ice wedge, whereas the middle part shows $\delta^{18}\text{O}$ of -30 ‰ and d of up to 6 ‰. Segregated ice has a low mean $\delta^{18}\text{O}$ of -23.4 ‰ and d of -0.4 ‰, respectively (Tab. 2). The observed changes of $\delta^{18}\text{O}$, d and conductivity indicate exchange processes from the enclosing sediment to the ice wedge. The hydrochemical (and isotopic) gradient between the ice wedge and segregated ice is partly compensated during the existence of the 42 kyr old ice wedge. It is important to note that this effect is only found in some Ice Complex ice wedges. SOLOMATIN (1986) postulated, a migration of moisture from the host sediment towards the ice wedge was caused by differences in heat capacities and dilation coefficients of ice and ice-rich sediment. As a consequence, small cracks are formed at the sides of an ice wedge and filled with water. This process indicates the possibility of moisture exchange in the contact zone between an ice wedge and the sediment, which could compensate hydrochemical and isotopic gradients. The transfer of water molecules in permafrost depends on composition and structural characteristics of soil and water. YERSHOV (1998) emphasises that the migration of bound water in frozen ground is driven by potential differences (such as temperature or ion concentration). Only in the case of soil pores relatively empty of water and ice must vapour transfer be considered. We conclude that in the fine-grained and ice-rich Ice Complex, water migration is the

driving force for the isotope and ion exchange between ice wedge and segregated ice, which was identified for the first time by means of stable isotopes and hydrochemistry.

PALEOCLIMATIC EVOLUTION AS REVEALED FROM STABLE ISOTOPE DATA

A wide range of hydrogen and oxygen isotopic compositions is observed for ice wedges on the Bykovsky Peninsula. Stable isotope minimum, mean and maximum values, standard deviation for 15 ice wedges of the three genetic units on the Bykovsky Peninsula Ice Complex (8 ice wedges), alas (3) and log (4) are presented in Table 2. Additionally, the slope and the intercept in the $\delta^{18}\text{O}$ - δD diagram as well as the sampling heights (a.s.l.) and the widths of all ice wedges are given. Variations in δD and $\delta^{18}\text{O}$ of 100 ‰ and 11.5 ‰, respectively, were measured for all ice wedges, with a mean isotopic composition of $\delta\text{D} = -218.0$ ‰ and $\delta^{18}\text{O} = -28.4$ ‰. This reflects changing, but always very cold climatic conditions in the working area during winter.

For some ice wedges (e.g. MKh-3 in the Ice Complex) horizontal and vertical transects were sampled. Stable isotopes of vertical transects of ice wedges show up to four times lower standard deviations than horizontal transects, because vertical sampling (Fig. 4) is carried out along the cracking direction (following one vein). Therefore, a randomly sampled vertical profile does not necessarily reflect climatic trends.

In earlier studies, small and medium-sized ice wedges were considered to be important for paleoclimate, stratigraphic and genetic studies (VAIKMÄE 1991). Because of the possibility of exchange processes between ice wedges and the enclosing sediments, as discussed above, we chose a statistical approach for a paleoclimatic reconstruction, using big ice wedges of the Ice Complex. Eliminating the samples influenced by segregated ice and using mean values and ranges for horizontal sampling transects of ice wedges, we expect to find isotopic trends, which in a second step could be attributed to climatic variability, especially to changes in winter temperatures. The variability within an ice wedge surely also contains climatic information, but it is difficult to attribute an ice vein to a discrete year.

The differences in mean $\delta^{18}\text{O}$ and δD of Ice Complex, alas and log ice wedges represent the development of mean winter temperatures throughout time (Figs. 8a-8d). In general, samples from the Pleistocene Ice Complex show an isotopic composition of -29 ‰ to -32 ‰ for $\delta^{18}\text{O}$ and of -230 ‰ to -250 ‰ for δD . The mean $\delta^{18}\text{O}$ values of all Pleistocene Ice Complex ice wedges are between -33 ‰ and -29.5 ‰. Because of the close relationship between temperatures and isotopic composition, mean winter temperatures can be assumed as constantly relatively cold for the investigated time interval between 58-20 ka.

The lightest isotopic composition (as low as $\delta^{18}\text{O} = -33.9$ ‰ and $\delta\text{D} = -267.5$ ‰) is observed in the oldest Ice Complex ice wedges located close to sea level. We assumed that in the period of ice wedge formation (at about 60-55 ka), the mean annual winter temperatures must have been the lowest. Relatively heavy $\delta^{18}\text{O}$ and δD values for ice wedges of the Ice Complex of up to -25 ‰ and -190 ‰ are observed in the left

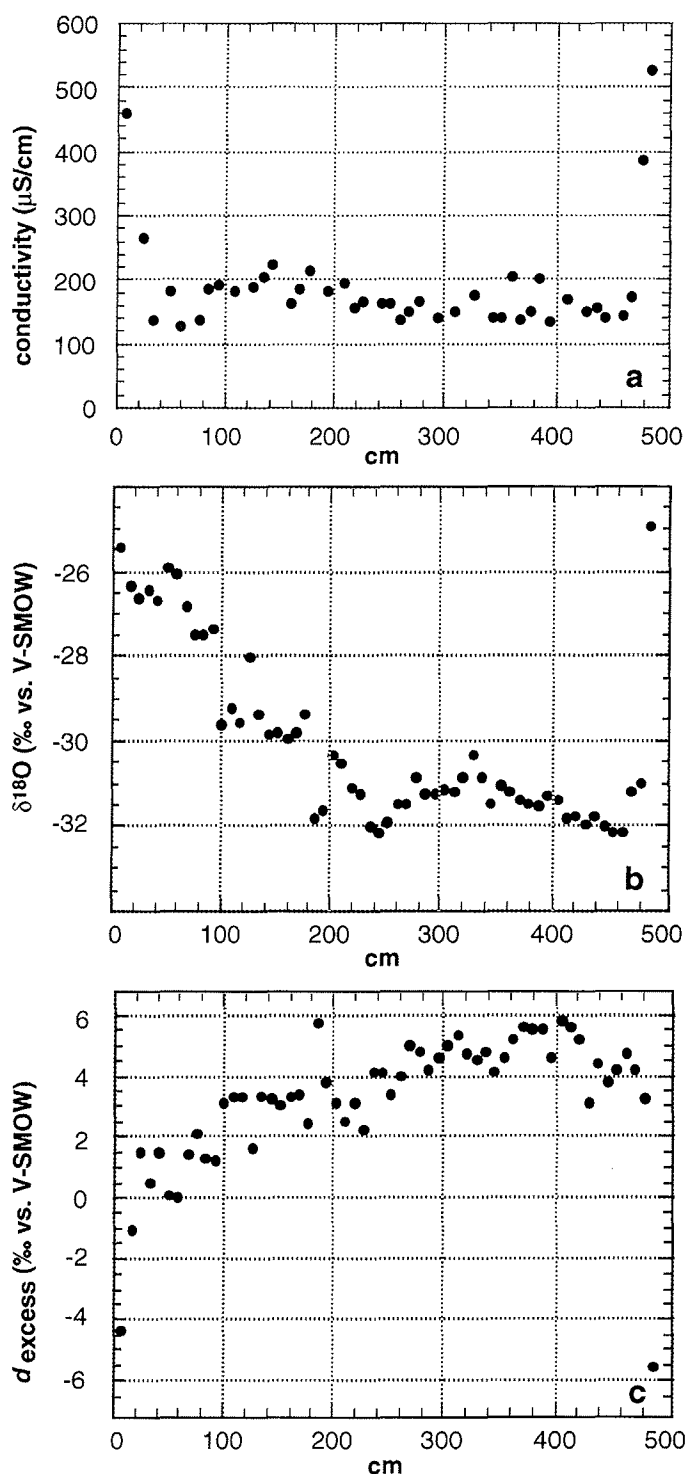


Fig. 7: Electrical conductivity (a), $\delta^{18}\text{O}$ (b) and d excess (c) of 5 m long horizontal sampling transect of Pleistocene ice wedge MKh-3 (height 11.1 m a.s.l.). For the location of the sampling transect in the outcrop see Fig. 3; for general sampling scheme see Fig. 4.

Abb. 7: Elektrische Leitfähigkeit (a), $\delta^{18}\text{O}$ (b) und d excess (c) für einen 5 m langen horizontalen Probenahme-Transsekt des pleistozänen Eiskeils MKh-3 (Höhe: 11.1 m). Schema der Probenahme-Schnittes in Abb. 3.

half of the upper horizontal transect of ice wedge MKh-3 (Fig. 7b). Only in parts, this could be attributed to exchange processes between ice wedge and adjacent sediment. Conse-

Ice wedge	Remarks	N	height a.s.l. (m)	width (m)	$\delta^{18}\text{O}$ (‰) min.	$\delta^{18}\text{O}$ (‰) mean	$\delta^{18}\text{O}$ (‰) max.	$\delta^{18}\text{O}$ (‰) s.d.	δD (‰) min.	δD (‰) mean	δD (‰) max.	δD (‰) s. d.	d (‰) min.	d (‰) mean	d (‰) max.	d (‰) s. d.	slope	intercept	R ²
LOG																			
MKh-1.1	complete ice wedge	5	17.0-16.5	0.5	-28.93	-27.79	-26.39	1.06	-216.8	-208.0	-197.4	8.0	13.7	14.3	15.0	0.5	7.58	2.7	0.99
MKh-1.3	complete ice wedge	10	17.5-16.9	0.8	-29.02	-26.27	-23.32	1.86	-217.3	-197.3	-173.8	14.7	9.9	12.8	14.8	1.3	7.86	9.1	0.99
MKh-1.6	complete ice wedge	5	20.0-19.4	0.5	-25.08	-23.64	-22.52	1.05	-189.2	-177.1	-168.5	8.6	11.3	12.1	13.4	0.9	8.12	14.8	0.99
MKh-4.13 (Hol.)	Holocene part	19	23.9-22.5	0.8	-26.96	-25.79	-24.01	0.83	-206.0	-194.0	-179.8	6.7	8.8	12.3	13.9	1.1	7.99	12.0	0.97
ALAS																			
BYK-H	complete ice wedge	15	5.1	1.5	-29.07	-26.14	-24.14	1.50	-219.6	-197.7	-182.8	11.3	8.5	11.4	13.0	1.2	7.51	-1.3	0.99
BYK-A1 (Hol)	Holocene part	6	0.8	3.0	-28.72	-28.26	-27.89	0.38	-213.8	-210.6	-207.7	2.6	14.1	15.5	16.2	0.8	6.55	-25.6	0.94
BYK-A2	complete ice wedge	109	4.5-2.1	3.3	-30.16	-28.18	-23.73	1.07	-224.3	-210.9	-177.1	7.6	10.7	14.5	17.8	1.5	7.08	-11.5	0.98
BYK-A2	upper horizontal transect	36	4.5	3.6	-30.16	-27.95	-23.73	1.13	-224.3	-209.3	-177.1	8.2	11.3	14.3	17.0	1.6	7.19	-8.5	0.98
BYK-A2	lower horizontal transect	59	2.5	2.7	-30.09	-28.25	-24.44	1.11	-224.0	-211.4	-184.1	7.9	10.7	14.6	17.8	1.5	7.00	-13.6	0.98
BYK-A2	vertical transect	14	4.5-2.1	-	-29.38	-28.46	-27.23	0.53	-219.7	-212.9	-203.8	3.9	13.0	14.8	16.1	0.7	7.32	-4.5	0.97
ICE COMPLEX																			
MKh-4.6	complete ice wedge	50	37.2-36.2	3.0	-30.03	-25.76	-23.07	1.67	-232.6	-195.7	-174.5	13.9	7.5	10.4	12.6	1.4	8.31	18.3	0.99
MKh-00	complete ice wedge	35	30.0	3.5	-31.08	-29.52	-28.16	0.80	-243.9	-230.2	-217.7	7.8	1.9	6.0	9.1	1.8	9.53	51.3	0.97
MKh-4.13 (Pleist)	Pleistocene part	36	22.5-21.5	3.5	-32.12	-31.17	-28.28	0.71	-253.5	-245.0	-221.8	5.8	3.2	4.4	5.7	0.6	8.24	11.9	0.99
MKh-5	horizontal transect	72	19.7-19.0	3.5	-31.89	-30.80	-29.25	0.61	-250.4	-241.3	-228.8	5.0	3.4	5.0	6.5	0.6	8.16	9.9	0.99
MKh-3	complete ice wedge	112	12.75-8.35	5.0	-32.27	-30.09	-24.97	1.86	-253.2	-237.3	-205.4	13.0	-5.6	3.3	6.5	2.2	6.96	-27.9	0.99
MKh-3	upper horizontal transect	48	11.1	5.0	-32.15	-30.41	-25.91	1.64	-253.1	-239.6	-207.2	11.9	0.0	3.7	5.8	1.5	7.28	-18.2	1.00
MKh-3	lower horizontal transect	21	9.1	3.1	-31.06	-29.74	-27.56	1.13	-244.4	-235.1	-219.9	8.2	0.0	2.7	4.5	1.3	7.22	-20.1	0.99
MKh-3	vertical transect	23	12.75-8.35	-	-32.27	-31.42	-30.32	0.58	-251.7	-246.2	-238.1	3.8	2.8	5.2	6.5	1.0	6.50	-42.0	0.98
MKh-1.2	complete ice wedge	49	3.0	4.5	-33.92	-31.56	-30.02	0.94	-267.5	-247.9	-232.3	8.1	2.7	4.6	7.9	1.0	8.54	21.7	0.99
MKh-1.2	horizontal transect	45	3.0	4.5	-33.92	-31.63	-30.02	0.95	-267.5	-248.5	-232.3	8.1	2.7	4.5	7.9	1.0	8.54	21.7	0.99
MKh-1.2	vertical transect	5	2.8-3.6	-	-30.81	-30.73	-30.47	0.15	-242.1	-240.9	-238.1	1.6	4.3	4.9	5.7	0.5	10.90	94.2	0.98
BYK-A1 (Pleist)	Pleistocene part	6	0.8	2.0	-33.41	-32.71	-31.44	0.71	-262.2	-256.8	-247.2	5.3	4.1	4.9	5.4	0.6	7.50	-11.5	0.99
MKh-00-10	complete ice wedge	18	0.5	3.0	-32.53	-31.55	-30.53	0.52	-259.2	-251.7	-244.5	4.0	-0.4	0.7	2.1	0.8	7.45	-16.7	0.96
SEGREGATED ICE		66			-30.45	-23.42	-17.72	3.25	-231.7	-187.7	-134.8	24.9	-11.7	-0.4	15.6	7.8	7.33	-16.1	0.91
RECENT WATER																			
Rain water		10			-16.97	-14.80	-11.43	1.95	-132.6	-115.7	-91.4	13.4	-3.4	2.7	6.1	3.2	6.77	-15.5	0.98
Snow patches		9			-27.5	-23.19	-19.74	3.01	-211.2	-176.2	-149.8	24.3	6.2	9.3	13.4	2.2	8.01	9.6	0.99

Tab. 2: Stable isotope ($\delta^{18}\text{O}$, δD and d excess) minimum, mean and maximum values, standard deviations (s. d.), as well as slopes and intercepts in the $\delta^{18}\text{O}$ - δD diagram for all ice wedges of three genetic units Ice Complex, alas and log.

Tab. 2: Minimal-, Mittel-, Maximalwerte und Standardabweichungen (s. d.) für Sauerstoff- und Wasserstoff-Isotope ($\delta^{18}\text{O}$, δD and d excess), sowie Steigung und Schnittpunkt im $\delta^{18}\text{O}$ - δD -Diagramm aller Eis-keile für die drei genetischen Einheiten Eis-Komplex, Alass und Log.

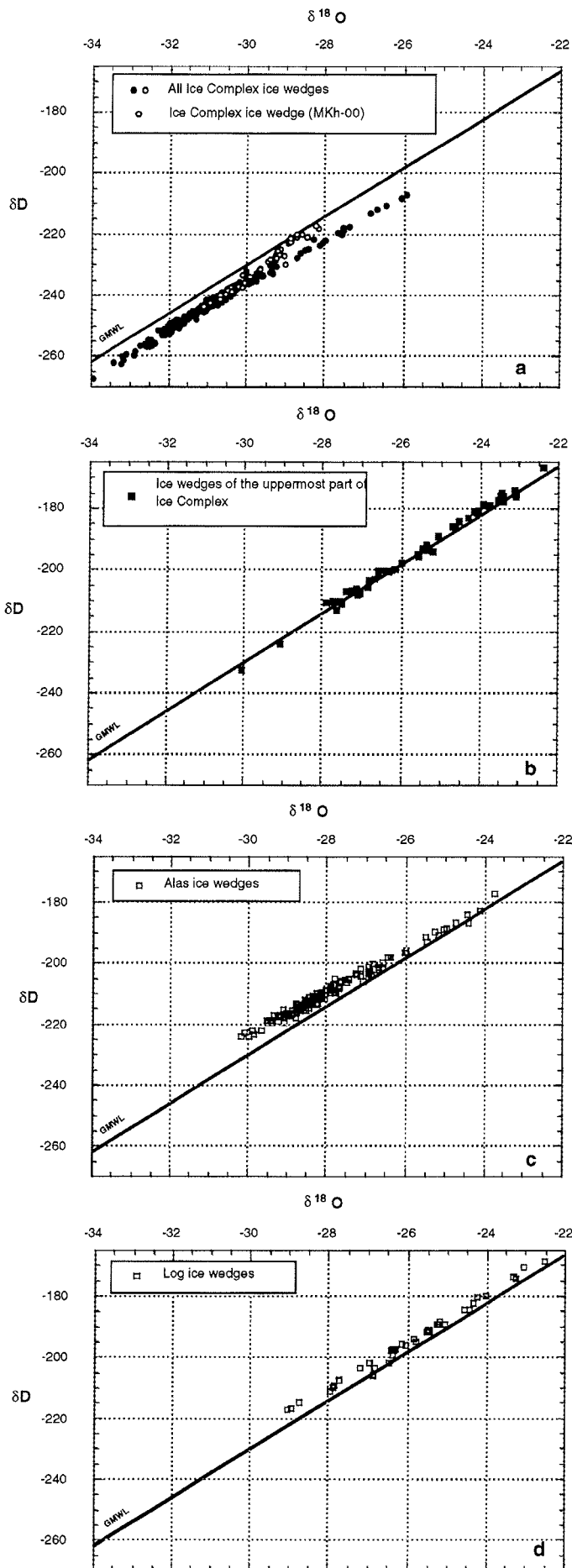


Fig. 8: $\delta^{18}\text{O}$ - δD diagrams for ice wedges in all genetic units. (a) Late Pleistocene part of the Ice Complex. Samples of the ice wedge Mkh-00 are represented by white dots; (b) uppermost part of the Ice Complex (ice wedge MKh-4.6); (c) Alas; (d) thermo-erosional valley (Log). GMWL is the Global Meteoric Water Line.

Abb. 8: $\delta^{18}\text{O}$ - δD -Diagramme für Eiskeile aller genetischen Einheiten: (a) Spätpleistozäner Teil des Eiskomplexes. Die Proben aus Eiskeil Mkh-00 sind mit weißen Punkten gekennzeichnet; (b) Oberster Bereich des Eiskomplexes (Eiskeil MKh-4.6); (c) Alas; (d) Thermoerosionstal (Log). GMWL ist die globale meteorische Wasserlinie.

quently, during the formation of this part of ice wedge MKh-3, less severe winter temperatures can be assumed.

Relatively constant cold climatic conditions according to the mean values varying between -31.2‰ and -29.5‰ for $\delta^{18}\text{O}$ and -245‰ and -230‰ for δD are characteristic for the next younger ice wedge transects (MKh-5, MKh-4.13, MKh-00) between about 26-20 ka. All samples of the Late Pleistocene Ice Complex (Fig. 8a) lie on a straight line parallel to the GMWL and in general show low d excess values of 0-5 ‰. The mean d excess is constantly between 3.7-5.0 ‰. Samples of MKh-00 (30 m a.s.l.) exhibit a different signature. They show an isotopic range, which seems to be typical for the Ice Complex, but a slope in the $\delta^{18}\text{O}$ - δD diagram of 9.5 and a mean d excess of 6.0 ‰ are higher than for all previously formed Ice Complex samples. The steep slope is apparently caused by a change from low to high d excess, which will be discussed later.

Ice wedge MKh-4.6 (36 m a.s.l.) in the uppermost part of the Ice Complex represents a special case (Fig. 8b). The $\delta^{18}\text{O}$ and δD values range mostly between -28‰ and -23‰ and -210‰ and -270‰ , respectively, with mean values of -25.8‰ and -196‰ indicating much warmer winters than before. All samples plot on the GMWL, with a high mean d excess of about 10.4 ‰. In the $\delta^{18}\text{O}$ - δD diagram, a slope of 8.3 indicates no significant evaporation effects.

In Figures 8c and 8d, all samples for the younger genetic units, alas and log are displayed. The $\delta^{18}\text{O}$ values are generally significantly heavier than in the Ice Complex, but similar to those in Figure 8b ranging from -30‰ to -24‰ for the alas and -29‰ to -22.5‰ for the log. Thus, a similar range of winter temperatures is reflected. For the formation of log ice wedges, winters might have been slightly warmer, as indicated by mean $\delta^{18}\text{O}$ and δD . d excess values of both Holocene genetic units are in general higher than 10 ‰ pointing to a similar source for winter precipitation as for the uppermost part of Ice Complex. Log ice wedges are characterised by a mean slope close to 8 in the $\delta^{18}\text{O}$ - δD diagram, whereas alas ice wedges have lower slopes of about 7.0. The latter evidently points to the participation of water, which has been subject to evaporation effects before the formation of ice veins. Both ice wedges located close to the slope near the Ice Complex (BYK-A2 and BYK-A1) show these effects, whereas BYK-H situated at greater distance is different (lower d , $\delta^{18}\text{O}$ and δD and higher slope of 7.5). Thus, mixing of snow meltwater with surface water from slopes has to be taken into account for the formation of BYK-A1 and BYK-A2. Both log ice wedges containing tritium (MKh-1.6, MKh-1.3) show differences in isotopic composition of up to 2.5 ‰ in $\delta^{18}\text{O}$ and 20 ‰ in δD , which may be explained by the small number ($N = 5$) of samples measured.

In Figure 9, the development of $\delta^{18}\text{O}$, δD and d excess of all Ice Complex ice wedges (without samples evidently influenced by exchange processes) are displayed for the interval between 10-60 ka. The differences between mean and median are in general negligible, except for the upper horizontal transect of MKh-3.

The development of the Ice Complex can be subdivided into three intervals. The coldest period (Ia) was between 60-55 ka as indicated by low stable isotope values in ice wedges,

followed by a slight rise of winter temperatures. This trend is supported by pollen data (ANDREEV et al. 2002) and sediment analysed from the Mamontovy Khayata section on Bykovsky Peninsula (SCHIRRMESTER et al. submitted, SIEGERT et al. 2002). Period (Ib) between about 45-22 ka is characterised by very stable, still cold winter conditions as indicated by low $\delta^{18}\text{O}$, δD and d excess. Both, pollen and sediment data as well as numerous soil horizons in the middle level of the Ice Complex show strong variations of the paleoenvironmental conditions at that interval. From 40-30 ka, the highest number of

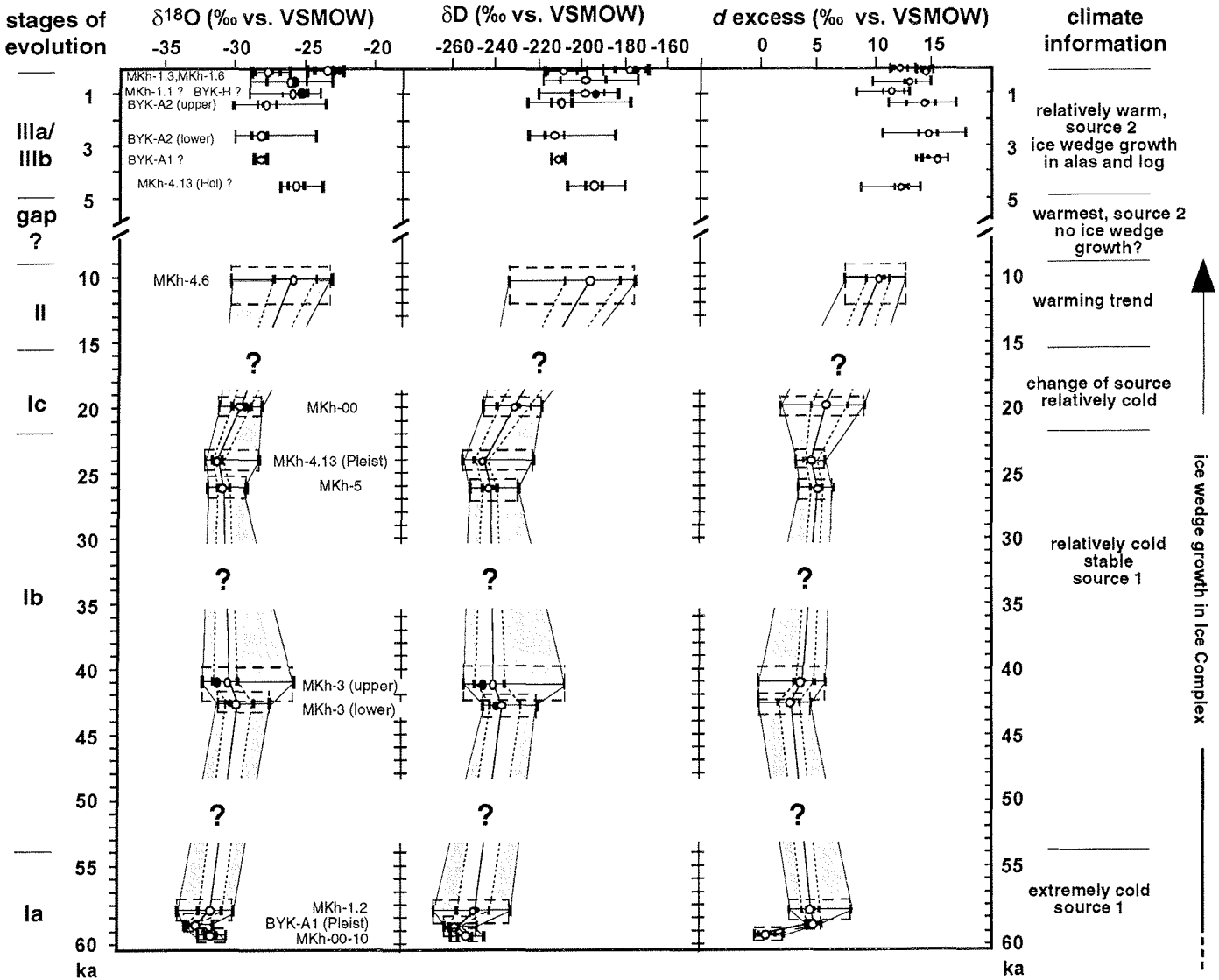


Fig. 9: Development of $\delta^{18}\text{O}$, δD and d excess of all Ice Complex ice wedges (without samples evidently influenced by exchange processes) and for the younger units alas and log through time. White dots are the mean isotopic composition, black dots the median of horizontal transects. A straight black line follows the development of the mean isotopic composition through time. The respective range (grey field) and an intermediate area (white field) between the quartiles Q1 and Q3 (dotted lines) are held out for visualisation. A (white or black) dot does not correctly represent a horizontal ice wedge transect, because for horizontal ice wedge growth a time span is also needed. Therefore, estimated ages as calculated above are displayed for the horizontal time information of ice wedges (dashed squares). White gaps were left where no ice wedges were sampled. Additionally, Holocene ice wedges are displayed. When no age determinations were available, ice wedges were put into a „logical“ order (marked with „?“).

Abb. 9: Zeitliche Entwicklung von $\delta^{18}\text{O}$, δD und d excess für alle Eiskeile aus dem Eis-Komplex (ohne Proben, die durch Austauschprozesse zwischen Eiskeil und Sediment beeinflusst sind) und für die jüngeren Einheiten Alass und Log. Die Mittelwerte der Isotopenzusammensetzung (weisse Punkte) sind zur Visualisierung durch eine schwarze Linie verbunden, schwarze Punkte kennzeichnen den Median für horizontale Probenahme-Transsekte. Zusätzlich sind die Variationsbreite (grauer Bereich) und der Bereich (weiß) zwischen den Quartilen Q1 und Q3 (gestrichelte Linie) dargestellt. Die geschätzten Altersinformationen (siehe Text) für horizontale Probenahme-Transsekte sind durch gestrichelte Quadrate gekennzeichnet. Die Lücken im Diagramm sind auf fehlende Proben aus den entsprechenden Altersstufen zurückzuführen. Zusätzlich sind die holozänen Eiskeile in „logischer“ chronologischer Abfolge dargestellt, undatierte Eiskeile sind mit „?“ markiert.

insect and mammal remains were found, pointing to favourable conditions for fauna and flora (SIEGERT pers. comm.). After 22 ka, a rise in d excess is observed in Ice Complex ice wedges proceeding to the Holocene. This stage Ic was relatively cold in winter and reflects changing climatic conditions in the source of precipitation. The Late Pleistocene cold period (or Sartanian in Russian stratigraphy), reflected in pollen from 26-16 ka, is apparently not reflected in the isotopic composition of ice wedges. This may be due to missing samples for that time slice. A strong rise in the mean $\delta^{18}\text{O}$ of 5 ‰ and in δD of 25 ‰ is observed for the Pleistocene-Holocene transition. The rise in δ values is also well known from Greenland (GROOTES et al. 1993) and Antarctic ice cores (PETIT et al. 1999). Period (II) is interpreted as a transitional stage with climate warming. The trend of a rise in $\delta^{18}\text{O}$ in ice wedges from the Bykovsky Peninsula has already been measured by FUKUDA (1994), albeit with a much lower resolution. A gap in ice wedge growth is indicated by a lack of data from about 8-4.5 ka. Limited or missing ice wedge growth during that time was presumably caused by the occurrence of extensive lakes (SCHIRRMESTER et al. submitted). According to ANDREEV et al. (2002), the highest amount of tree pollen data was found in the sediment from 8.2-4 ka indicating a most favourable climate or the „Holocene climatic optimum“ at this time interval. Additionally, numerous tree remains from this time were found in Northern Siberia (SIEGERT et al. 1999). Despite insecure age estimates for some ice wedges, two overlapping stages (IIIa and IIIb) of ice wedge growth in log and alas can be distinguished for the second half of the Holocene. Both show similar climatic situations, which is confirmed by pollen data (ANDREEV et al. 2002). Nevertheless, alas ice wedges reflect slightly colder winters than log ice wedges. After 4.5 ka, climate deterioration and drying up of lakes is known from Taymyr Peninsula, Northern Siberia (SIEGERT et al. 1999), which is followed by new ice wedge growth (FRENCH 1996).

SOURCES

The existence of a strong linear correlation ($R^2 = 0.99$) of all Ice Complex ice wedges (except MKh-00 and MKh-4.6) in the $\delta^{18}\text{O}$ - δD diagram clearly indicates that ice wedge growth is only weakly influenced by fractionation processes. Only in the contact zone between ice wedge MKh-3 (Fig. 7a-c) and adjacent sediment, water from the segregated ice formerly subjected to evaporation has been transferred to the ice wedge leading to a deviation from the linear correlation towards a lower slope in the $\delta^{18}\text{O}$ - δD diagram. We conclude that fractionation during melting and winter sublimation of snow, which would both lead to a shift in d excess, must have been of small influence during Ice Complex ice wedge growth. This leads to the assumption that first meltwater feeds the frost crack. Additionally, the main source of the precipitation incorporated in ice wedges on the Bykovsky Peninsula must have been constant, or, in the case of two or more different sources, their relative amount. Another explanation for the strong linear correlation of Ice Complex and other ice wedges could be diffusion within the ice wedge. The stable isotope records of $\delta^{18}\text{O}$ and δD in ice cores show that the isotopic gradients are smoothed with time by diffusion (JEAN-BAPTISTE et al. 1998). Transport of hydrogen and oxygen atoms through solid ice is slow, whereas water vapour diffusion through the interconnected porosity is much faster. Diffusion in ice wedges

would be supported by (i) small variations and the absence of abrupt shifts in the isotopic composition of two adjacent samples and (ii) lower correlation in younger ice wedges because of limited time for „isotopic smoothing“. But all analysed ice wedges have very high correlation coefficients (Tab. 2) showing no increasing „smoothing“ with time. To prove this, a closer view of the differences in the isotopic composition between single veinlets is necessary.

For the shift in d excess between the Pleistocene and the Holocene, various explanations are possible. First, a change of the main source for the precipitation or a change of the pathways may have led to a higher d excess in the Holocene (and Latest Pleistocene). The source of the winter precipitation today is probably located in the Northern Atlantic. The western air transfer dominates all over Northern Eurasia (RINKE et al. 1999), fed by Atlantic moisture (KUZNETSOVA 1998). Especially in January, the Siberian anticyclone remains in a stable position over the Arctic Ocean, north of the Laptev Sea. The Arctic Ocean is frozen in winter, leaving only a thin polynya with open water. In coastal regions this polynya has to be taken into account as a moisture source. Continental areas of Northern Siberia with open water are also frozen in winter, but the low temperatures in the Arctic regions impede the moisture transfer to the atmosphere. Moreover, a large amount of snow originating from a source with reprecipitated water is detectable in the $\delta^{18}\text{O}$ - δD diagram by a low slope. The advection of moisture from the Pacific Ocean is restricted by atmospheric circulation patterns and the mountain relief (LEROUX 1993). Therefore, the boundary between regions influenced by Pacific and Atlantic moisture is situated far to the East between 130° E and 150° E. In winter, the lowest moisture content is observed in this area and eastern moisture transport in the North of the Aleutian depression from the Pacific meets Atlantic air masses (KUZNETSOVA 1998). Nevertheless, the Pacific can be ruled out, because the present climatic conditions on the Bykovsky Peninsula are similar to those on the Taymyr Peninsula (BOIKE 1997), with snow presumably deriving from the same moisture source (see above). Additionally, according to (CLARK & FRITZ 1997), Atlantic marine-influenced stations in Northern Canada today have a much higher d excess (about 10.6 ‰) than Pacific marine-influenced stations ($d = 3.6$ ‰).

Little is known about past Arctic atmospheric circulation. But, Atlantic derived precipitation was presumably influenced by two major changes in the paleoenvironmental history: the existence of ice sheets covering large areas of Western Siberia during periods in the Weichselian (SVENDSEN et al. 1999), and the more continental position of the working area with respect to the sea (ALEKSEEV 1997).

A higher continentality is generally accompanied by a larger amplitude of temperatures. Therefore, marine-influenced precipitation has a narrower range of isotopic composition compared to continental areas (CLARK & FRITZ 1997) and consequently higher $\delta^{18}\text{O}$ and δD in the ice wedges. During the late glacial maximum (LGM, 15-18 ka ^{14}C), the sea level was much lower than today and the Arctic shelves were subaerially exposed. A distance from the Bykovsky Peninsula to the sea of about 500 km (ROMANOVSKIJ et al. 1999) has been estimated. „Colder“ winter temperatures are not indicated by the stable isotopic composition of ice wedges during the Sartanian cold

period. Thus, continentality does not seem to have a major influence on winter temperatures. BREZGUNOV et al. (1998) correlated $\delta^{18}\text{O}$ of precipitation with mean monthly temperatures at Russian meteorological stations. Their map shows latitudinal gradients and strong continentality effects on variations of $\delta^{18}\text{O}$ in precipitation for Northern Siberia. The Lena Delta area is located in the region with the lowest $\delta^{18}\text{O}$ values (-24 ‰), indicating a high degree of continentality even though presently it is close to the Laptev Sea coast.

The position and extent of a possible LGM ice sheet in Northern Siberia is still being controversially discussed (e.g. GROSSWALD 1998, GROSSWALD et al. 1999, ASTAKHOV 1998). The presence of the Ice Complex with syngenetic ice wedges, which were growing between >60-9 ka on the Bykovsky Peninsula are evidence for the absence of a large ice sheet in this area. But even the existence of a West Siberian LGM ice sheet should have had an influence on atmospheric circulation patterns and thus on the isotopic composition of precipitation. Any ice sheet must have acted as a morphological barrier changing the pathways of moisture transport, and blocking or deviating the Atlantic air masses. During the LGM, moist tropical air masses were forced northward both in the North Pacific and in the Atlantic regions (LEROUX 1993). Higher humidity in the source region leads to lower *d* excess. Consequently, both are possible source regions for moisture feeding our ice wedges. A change of the source of the precipitation from the Northern Pacific to the Atlantic after the decay of the LGM ice sheet is a possible explanation for the shift in *d* excess. A second possibility, is moisture originating from lower latitudes of the Atlantic (JOHNSON & WHITE 1989) which has been slightly colder during the LGM (CLIMAP 1976), combined with a southward displacement of the sea ice boundary. Despite the larger distance to the study area, colder sea surface temperatures or higher moisture in the source region may explain the low *d* excess in winter precipitation. On the Taymyr Peninsula, a rise in *d* excess is observed between Pleistocene and Holocene ice wedges (SIEGERT et al. 1999). We conclude that winter precipitation originated from the west, presumably at lower latitudes in the Atlantic.

Another possible explanation for the shift in *d* excess is related to the modification of isotopic composition in the snow cover feeding the frost cracks during spring. In the case of a very thin snow cover, the importance of sublimation, evaporation and diffusion within the snow cover as well as percolation of melt water through it would increase leading to a change in the *d* excess. After GASANOV (1977), sublimation of ice wedge ice may occur in an open frost crack and desublimation from a moist air mass in the upper part of the crack. This is caused by a gradient between low air temperature and higher permafrost temperature in winter. Cold air enters into the frost crack, where it becomes undersaturated in water vapour when the air temperature rises. Depending on humidity, this process could also change the *d* excess.

CONCLUSIONS

The following results were obtained during the study of ice wedges carried out on the Bykovsky Peninsula, Northern Siberia:

- The presence of ice wedges since more than 60 ka points to permafrost conditions and to the absence of a glacier cover in this area. For these remote non-glaciated areas of Northern Siberia, ice wedges are important climate archives for isotope studies.

- Ice wedges of three different genetic units and of different ages could be distinguished by means of oxygen and hydrogen isotopes. The Ice Complex was subdivided isotopically into a period of very cold winter temperatures between 60-55 ka, followed by a long stable period of cold winters from 50-24 ka. A rise of 5 ‰ in $\delta^{18}\text{O}$ and of 25 ‰ in δD probably after the Late Glacial Maximum indicates a climate warming trend.

- For the Ice Complex, a continuous age-height relationship of 0.7 m/ky was established, pointing to syngenetic freezing and relatively constant vertical ice wedge growth and sediment accumulation rates. Ice wedge growth was limited during the Holocene optimum, because of wide-spread lake formation processes. The following climate deterioration led to initial Holocene ice wedge growth (in alas) after 4.5 ka continuing until today at relatively warm winter temperatures as compared to the Pleistocene.

- The isotopic composition of old ice wedges may be altered by migration of water between the ice wedge and the enclosing segregated ice, which must be considered for paleoclimatic interpretation.

- The *d* excess of ice wedges contains information about the moisture source region for winter precipitation. A shift in the *d* excess after about 20 ka is probably related to a change of the main marine source of the precipitation. In the Pleistocene, the moisture source region, presently the North Atlantic, lay further to the south.

ACKNOWLEDGMENTS

This research is part of the project „System Laptev Sea 2000“ funded by the German Ministry of Education and Research (BMBF; project no. 03G0534). The authors thank Lutz Schirmer (AWI Potsdam) for valuable help and intensive discussions. From AWI in Potsdam, Helga Henschel is acknowledged for language revision of the manuscript, Thomas Kumke for help with statistics. The reviews of R. Spielhagen and R. Vaikmäe substantially improved this paper. This is a publication of the Alfred Wegener Institute for Polar and Marine Research. We used data of the NOAA (National Oceanic and Atmospheric Administration (climate data archive <http://www.ngdc.noaa.gov>).

References

- Alekseev, M.N. (1997): Paleogeography and geochronology in the Russian Eastern Arctic during the second half of the Quaternary.- *Quatern. Int.* 41/42: 11-15.
- Andreev, A.A., Schirmer, L., Siegert, Ch., Bobrov, A.A., Demske, D., Seiffert, M., Hubberten, H.-W. (2002): Paleoenvironmental changes in northeastern Siberia during the Upper Quaternary – Evidence from pollen records of the Bykovsky Peninsula.- *Polarforschung* 70: 13-25.
- Arkhangelov, A.A., Vaikmyae, R.A., Mikhalev, D.V., Punning, Ya.M. & Solomatina, V.I. (1986): Stratigraphic subdivision of syngenetic permafrost by means of oxygen-isotope analysis.- *Transactions (Doklady) of the USSR* 290 (2): 94-96.

- Astakhov, V. (1998): The last ice sheet of the Kara Sea: Terrestrial constraints on its age.- *Quatern. Int.* 45/46: 19-28.
- Atlas Arktiki (Atlas of the Arctic) (1985): In: A.F. TRESHNIKOV (ed.), G.U.G.K., Moscow (in Russian).
- Boike, J. (1997): Thermal, hydrological and geochemical dynamics of the active layer at continuous permafrost site Taymyr Peninsula, Siberia.- *Rep. Polar Res.* 242: 104 pp.
- Brezgunov, B.S., Yesikov, A.D., Ferronsky, V.I. & Sal'nova, L.V. (1998): Spatial-temporal variations of oxygen isotope composition in precipitation and river water of Northern Eurasia and their relation to temperature changes.- *Vodnye Resursy* 25, No. 1: 99-104 (in Russian).
- Burn, C.R., Michel, F.A. & Smith M.W. (1986): Stratigraphic, isotopic, and mineralogical evidence for an early Holocene thaw unconformity at Mayo, Yukon Territory.- *Canadian J. Earth Sci.* 23: 794-803.
- Chizhov, A.B. & Dereviagin, A.Yu. (1998): Tritium in Siberian permafrost.- *Permafrost: Proceedings, Seventh International Conference, Yellowknife, Canada, Collection Nordiana, Quebec*: 151-156.
- Clark, I.D., Fritz, P. (1997): *Environmental Isotopes in Hydrology*.- Lewis Publishers. Boca Raton: 328 pp.
- CLIMAP Project Members (1976): The surface of the Ice-Age earth.- *Science* 191: 1131-1137.
- Craig, H. (1961): Isotopic variations in meteoric waters.- *Science* 133: 1702-1703.
- Dansgaard, W. (1964): Stable isotopes in precipitation.- *Tellus* 16: 436-468.
- Dereviagin, A.Yu., Meyer, H., Chizhov, A.B., Hubberten, H.-W. & Simonov, E.F. (2002): New data on the isotopic composition and evolution of modern ice wedges in the Laptev Sea region.- *Polarforschung* 70: 27-35.
- Epstein, S. & Mayeda, T. (1953): Variations of O18 content of waters from natural sources.- *Geochim. Cosmochim. Acta* 4: 213-224.
- French, H.M. (1996): *The periglacial environment*.- 2nd Ed. London, Longman: 341 pp.
- Fukuda, M. (1994): Occurrence of Ice-complex (Edoma) in Lena River Delta region and Big Lhyavosky Island, High Arctic Eastern Siberia.- In: G. INOUE (ed.), *Proceedings, Second Symposium on the joint Siberian Permafrost Studies between Japan and Russia in 1993*, Tsukuba, Japan: 1-9.
- Gasanov, Sh.Sh. (1977): Sublimation redistribution of material in ice wedges.- *Problems Cryolithology* 6: 224-229 (In Russian).
- Grigoryev, M.N., Imayev, V.S., Imayeva, L.P. et al. (1996): Geology, seismicity and cryogenic processes in the arctic areas of western Yakutia.- *Yakut. Scientific Centre SD RAS*: 80 pp. (in Russian).
- Grootes, P.M., Stuiver, M., White, J.W., Johnsen, S. & Jouzel, J. (1993): Comparison of oxygen isotope records from the GISP2 and GRIP Greenland ice cores.- *Nature* 366: 552-554.
- Grosswald, M.G. (1998): Late Weichselian ice sheets in Arctic and Pacific Siberia.- *Quatern. Int.* 45/46: 3-18.
- Grosswald, M.G., Hughes, T.J. & Lasca, N.P. (1999): Oriented lake- and ridge assemblages of the Arctic coastal plains: glacial landforms modified by thermokarst and solifluction.- *Polar Record* 194: 215-230.
- International Permafrost Association (1998): *Multi-Language Glossary of Permafrost and Related Ground-Ice Terms*.- In: R. O. VAN EVERDINGEN (ed.), *The Arctic Institute of North America, Calgary, Canada*: 78 pp.
- Jean-Baptiste, P., Jouzel, J., Stievenard, M. & Ciais, P. (1998): Experimental determination of the diffusion rate of deuterated water vapor in ice and application to the stable isotopes smoothing of ice cores.- *Earth Planet. Sci. Lett.* 158: 81-90.
- Johnsen, S.J., Dansgaard, W., Clausen, H.B. & Langway, C.C. (1972): Oxygen isotope profiles through the Antarctic and Greenland ice sheets.- *Nature* 235: 429-434.
- Johnsen, S.J. & White, J. (1989): The origin of Arctic precipitation under present and glacial conditions.- *Tellus* 41B: 452-468.
- Jouzel, J., Alley, R.B., Cuffey, K.M., Dansgaard, W., Grootes, P., Hoffmann, G., Johnsen, S.J., Koster, R.D., Peel, D., Shuman, C.A., Stievenard, M., Stuiver, M. & White, J. (1997): Validity of the temperature reconstruction from water isotopes in ice cores.- *J. Geophys. Res.* 102 (C12): 26471-26487.
- Kunitzky, V.B. (1989): *Cryolithogenesis of the lower Lena*.- Permafrost Institute, Academy of Science USSR, Siberian Department, Yakutsk: 162 pp. (in Russian).
- Kuznetsova, L.P. (1998): Atmospheric moisture content and transfer over the territory of the former USSR.- In: T. OHATA et al. (eds.), *Second International Workshop on Energy and Water Cycle in GAME-Siberia, 1997*: 145-151.
- Lachenbruch, A.H. (1962): Mechanics of thermal contraction cracks and ice-wedge polygons in permafrost.- *Geol. Soc. Amer. Spec. Pap.* 70: 69 pp.
- Leroux, M. (1993): The Mobile Polar High: a new concept explaining present mechanisms of meridional air-mass and energy exchanges and global propagation of palaeoclimate changes.- *Global Planet. Change* 7: 69-93.
- MacKay, J.R. (1974): Ice-wedge cracks, Garry Island, Northwest Territories.- *Canadian J. Earth Sci.* 11: 1366-1383.
- MacKay, J.R. (1983): Oxygen isotope variations in Permafrost, Tuktoyaktuk peninsula area, Northwest Territories.- *Pap. Geol. Surv. Canada*, B. 18: 67-74.
- Mackay, J.R. (1992): The frequency of ice-wedge cracking (1967-1987) at Garry Island, western Arctic coast, Canada.- *Canadian J. Earth Sci.* 29: 236-248.
- Merlivat, L. & Jouzel, J. (1979): Global climatic interpretation of the deuterium-oxygen 18 relationship for precipitation.- *J. Geophys. Res.* 84: 5029-5033.
- Meyer, H., Dereviagin, A. & Syromyatnikov, I. (1999): Ground ice studies.- In: V. RACHOLD (ed.), *Expeditions in Siberia in 1998*. *Rep. Polar Res.* 315: 155-163.
- Meyer, H., Schönicke, L., Wand, U., Hubberten, H.-W. & Friedrichsen, H. (2000): Isotope studies of hydrogen and oxygen in ground ice - Experiences with the equilibration technique.- *Isot. Environ. Health Sci.* 36: 133-149.
- Michel, F.A. (1982): *Isotope investigations of permafrost waters in northern Canada*.- Ph.D. Thesis, Dept. of Earth Sciences, Univ. of Waterloo, Canada: 227 pp.
- Nagaoka, D. (1994): Properties of Ice Complex deposits in Eastern Siberia.- In: G. INOUE (ed.), *Proceedings, Second Symposium on the Joint Siberian Permafrost Studies between Japan and Russia 1993*, Tsukuba, Japan: 14-18.
- Oeschger, H. (1985): The contribution of ice core studies to the understanding of environmental processes.- In: C.C. LANGWAY Jr., H. OESCHGER & W. DANSGAARD (eds.), *Greenland Ice Core: Geophysics, geochemistry, and the environment*. Amer. Geophys. Union, Washington/DC, USA. *Geophys. Monograph* 33: 9-17.
- Petit, J.R., Jouzel, J., Raynaud, D., Barkov, N.I., Barnola, J.M., Basile, I., Bender, M., Chappellaz, J., Davis, M., Delaygue, G., Delmotte, M., Kotiyakov, V.M., Legrand, M. & Stievenard, M. (1999): Climate and atmospheric history of the past 420,000 years from the Vostok ice core, Antarctica.- *Nature* 399: 429-436.
- Rinke, A., Dethloff, K., Spekat, A., Enke, W. & Hesselbjerg Christensen, J. (1999): High resolution climate simulations over the Arctic.- *Polar Res.* 18(2): 143-150.
- Romanovskij, N.N. (1985): Distribution of recently active ice and soil wedges in the USSR. Field and theory; lectures in geocryology.- In: M. CHURCH & O. SLAYMAKER (eds.), Vancouver, BC, Canada. Univ. B.C. Press: 154-165.
- Romanovskij, N.N., Kholodov, A.L., Gavrilov, A.V., Tumskoy, V.E., Hubberten, H.-W., Kassens, H. (1999): Ice-bonded permafrost thickness in the eastern part of the Laptev Sea shelf (results of computer modelling).- *Kryosfera Semlya III*, No. 2: 22-32.
- Romanovskij, N.N., Hubberten, H.W., Gavrilov, A.V., Tumskoy, V.E., Tipenko, G.S., Grigoryev, M.N. & Siebert, C. (2000): Thermokarst and Land - Ocean Interactions, Laptev Sea Region, Russia.- *Permafrost Periglac.* 11: 137-152.
- Schirrmester, L., Siebert, C., Kunitsky V.V., Grootes, P.M. & Erlenkeuser, H. (submitted): Late Quaternary ice-rich permafrost sequences as a paleoenvironmental archive for Laptev Sea Region in Northern Siberia.- *Intern. J. Earth Sci.*
- Sher, A.V., Kaplina, T.N. & Ovander, M.G. (1987): Unified regional stratigraphic chart for the Quaternary deposits in the Yana-Kolyma lowland and its mountainous surroundings.- Explanatory Note, in: *Decisions of Interdepartmental Stratigraphic conference on the Quaternary of the East USSR*. Magadan: 29-69 (in Russian).
- Siebert, C., Dereviagin, A.Yu., Shilova, G.N., Hermichen, W.D. & Hiller, A. (1999): Paleoclimatic indicators from permafrost sequences in the Eastern Taymyr Lowland.- In: H. KASSENS, H.A. BAUCH, I. DMITRENKO, H. EICKEN, H.-W. HUBBERTEN, M. MELLES, J. THIEDE & L. TIMOKHOV (eds.), *Land-Ocean systems in the Siberian Arctic: dynamics and history*, Berlin, Springer: 477-499.
- Siebert, C., Schirrmester, L. & Babiy, O. (2001): The sedimentological, mineralogical and geochemical composition of Late Pleistocene permafrost deposits from the Ice Complex of the Bykovsky Peninsula, Northern Siberia.- *Polarforschung* 70: 3-11.
- Slagoda, E.A. (1993): *Genesis and microstructure of cryolithogenic deposits at the Bykovsky Peninsula and the Muostakh Island*.- Unpubl. Diss., Yakutsk, RAS Siberian Section, Permafrost Institute: 218 pp. (in Russian).
- Solomatina, V.I. (1986): *Petrogenesis of ground ice*.- Novosibirsk, Nauka: 215 pp.
- Stuiver, M., Reimer, P.J., Bard, E., Beck, J.W., Burr, G.S., Hughen, K.A., Kromer, B., McCormac, F.G., van der Plicht, J. & Spurk, M. (1998): INTCAL98 radiocarbon age calibration, 24000 - 0 cal BP.- *Radiocarbon* 40: 1041-1083.

- Svendsen, J.I., Astakhov, V.I., Bolshiyakov, D.Yu., Demidov, I., Dowdeswell, J.A., Gataullin, V., Hjort, C., Hubberten, H.-W., Larsen, E., Mangerud, J., Melles, M., Moeller, P., Saarnisto, M., Siegert, M.J.* (1999): Maximum extent of the Eurasian ice sheets in the Barents and Kara Sea region during the Weichselian.- *Boreas* 28: 234-242.
- Tomirdiuro, S.V., Arslanov, Kh.A., Chernen'kiy, B.I., Tertychnaya, T.V. & Prokhorova, T.N.* (1984): New data on formation of loess-ice sequences in Northern Yakutia and ecological conditions of mammoth fauna in the Arctic during the late Pleistocene.- *Doklady AN SSSR*, 278, 6: 1446-1449 (in Russian).
- Vaikmäe, R.* (1989): Oxygen isotopes in permafrost and ground ice - a new tool for paleoclimatic investigations.- 5th Working Meeting „Isotopes in Nature“, Proceedings, Leipzig: 543-553.
- Vaikmäe, R.* (1991): Oxygen-18 in permafrost ice.- International Symposium of the Use of Isotope Techniques in Water Resources Development. Vienna, Austria, March 1991.
- Vasil'chuk, Yu.K.* (1992): Oxygen isotope composition of ground ice.- Application to paleogeocryological reconstructions.- Vol. 1, Moscow, Russia: 420 pp.
- Vasil'chuk, Yu.K.* (1991): Reconstruction of the paleoclimate of the late Pleistocene and Holocene on the basis of isotope studies of subsurface ice and waters of the permafrost zone.- *Water Res.* 17 (6): 640-674.
- Vasil'chuk, Yu.K., van der Plicht, J., Jungner, H., Soininen, E. & Vasil'chuk, A.C.* (2000): First direct dating of Late Pleistocene ice wedges by AMS.- *Earth Planet. Sci. Lett.* 179: 237-242.
- Yershov, E.D.* (ed.) (1989): *Geocryology of the USSR*.- Moscow, Nedra, Vol. Middle Siberia: 415 pp.
- Yershov, E.D.* (1998): *General Geocryology*.- Studies in Polar Research. English Edition: Cambridge University Press: 580 pp.